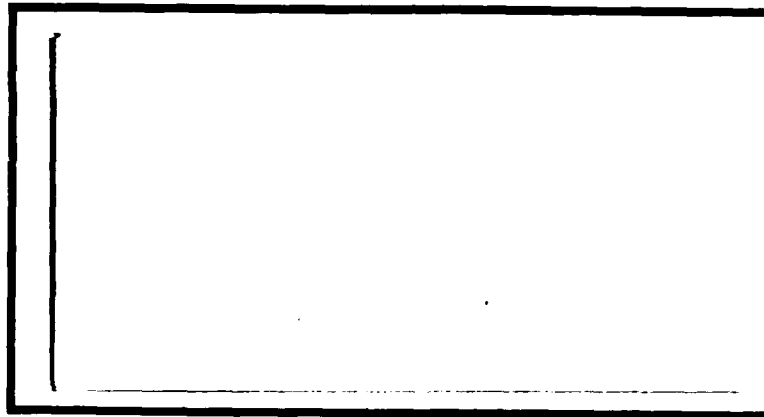


DTIC FILE COPY

(1)

AD-A202 604



DTIC
 ELECTE
 JAN 18 1989
 S D
 CD

DISTRIBUTION STATEMENT A
 Approved for public release
 Distribution Unlimited

DEPARTMENT OF THE AIR FORCE
 AIR UNIVERSITY

AIR FORCE INSTITUTE OF TECHNOLOGY

Wright-Patterson Air Force Base, Ohio

89 1 17 102

①

AFIT/EN/AA/88D-04

DTIC
ELECTE
JAN 18 1989
S D
D⁰³

OPTIMAL LOW THRUST TRAJECTORIES

FOR PLANETARY CAPTURE

THESIS

David E. Gaylor
Captain, USAF

AFIT/EN/AA/88D-04

Approved for public release; distribution unlimited

AFIT/GA/AA/88D-04

OPTIMAL LOW THRUST TRAJECTORIES
FOR PLANETARY CAPTURE

THESIS

Presented to the Faculty of the School of Engineering
of the Air Force Institute of Technology

Air University

In Partial Fulfillment of the
Requirements for the Degree of
Master of Science in Astronautical Engineering



David E. Gaylor, B.S.
Captain, USAF

December 1988

Accession For	
NTIS GRA&I	<input checked="" type="checkbox"/>
DTIC TAB	<input type="checkbox"/>
Unannounced	<input type="checkbox"/>
Justified	<input type="checkbox"/>
By	
Dist	
Availability Codes	
Dist	Avail and/or
A-1	

Approved for public release; distribution unlimited

Acknowledgements

I would like to express my appreciation to my advisor, Dr. Wiesel, whose guidance was instrumental to this effort. I would also like to thank the other members of my committee, Capt Bain and Capt Planeaux for their advice.

Table of Contents

Acknowledgements	ii
List of Figures	iv
Abstract	v
I. Introduction	1
II. Theory	4
The Restricted Three Body Problem	4
Regions of Motion and Capture Criterion	11
The Optimal Control Law	17
Two Point Boundary Value Problem	22
III. Results and Discussion	26
In the Vicinity of L_2	27
Case 1	32
Case 2	33
Case 3	38
Case 4	39
IV. Conclusions	45
Bibliography	47
Vita	48

List of Figures

Figure	Page
1. Coordinate System for Restricted Three Body Problem	5
2. Curves Of Zero Velocity for $\mu = 0.01$	14
3. Curves of Zero Velocity for $\mu = 0.1$	14
4. Curves of Zero Velocity for $\mu = 0.3$	15
5. Curves of Zero Velocity for $\mu = 0.5$	15
6. The Jacobi Integral along the X-axis for various μ	16
7. Periodic Orbit in Earth/Moon System	28
8. Trajectory for Case 1	34
9. Theta (degrees) vs Time for Case 1	35
10. Trajectory for Case 2	36
11. Theta (degrees) vs Time for Case 2	37
12. Trajectory for Case 3	41
13. Theta (degrees) vs Time for Case 3	42
14. Trajectory for Case 4	43
15. Theta (degrees) vs Time for Case 4	44

Abstract

The purpose of this study is to find optimal low thrust capture trajectories in the restricted three body problem. The region of phase space which corresponds to capture by a body is bounded by the curve of zero velocity passing through the equilibrium point (Lagrange point) L_2^{π} . If the spacecraft is driven to rest at L_2^{π} , capture has been achieved by adding the least amount of energy. An optimal control law is developed to achieve this based on maximizing the Jacobi integral. The dynamics are then linearized around L_2^{π} for the Earth/Moon system and the shooting method is used to solve the two point boundary value problem. This problem was found to be singular so the shooting method was modified to avoid making corrections along the null eigenvector. Four trajectories were found which demonstrate the optimal control law successfully caused the spacecraft to be captured by the Moon. *theses. figure*

OPTIMAL LOW THRUST TRAJECTORIES FOR PLANETARY CAPTURE

I. Introduction

Optimal trajectories for low thrust spacecraft have been the subject of study since the early 1960's. The majority of the previous studies concentrated on finding optimal transfer orbits in the classical two body problem. This study will be concerned with locating optimal capture trajectories for low thrust spacecraft in the restricted three body problem. For this study, a low thrust spacecraft is defined as having engines which produce less thrust than the force of local gravity.

When the U.S. space station becomes operational, the use of low thrust vehicles will become a practical means of interplanetary travel. Ion engines, which produce constant low thrust at high specific impulse, are ideal for transporting large payloads between planets.

The problem of interplanetary travel may be viewed as a series of capture problems. The purpose of this study is to find optimal low thrust capture trajectories in the restricted three body problem. The equations of motion for a thrusting spacecraft in the restricted three body problem are developed and the unforced motion is examined to

are developed and the unforced motion is examined to determine a criterion for capture.

For the unforced motion, an integral of the motion, the Jacobi integral is introduced. From this integral of the motion, curves of zero velocity are defined. These curves determine if motion is possible given the value of the Jacobi integral. The region of phase space which corresponds to capture by a body is bounded by the curve of zero velocity passing through the equilibrium point (Lagrange point) L_2 . This is the point where the two capture regions touch. If the spacecraft is driven to rest at L_2 , capture has been achieved by adding the least amount of energy.

An optimal control law is developed to achieve this based on maximizing the Jacobi integral. The resulting two point boundary value problem has no closed form solution, so a numerical solution is developed. The dynamics are then linearized around L_2 for the Earth-Moon system and the shooting method is used to solve the two point boundary value problem.

This problem was found to be singular so the shooting method was modified to avoid making corrections along the null eigenvector. Four cases are investigated. Case 1 demonstrated the modified shooting method was able to solve the two point boundary value problem if the initial

conditions were very close to the nominal initial conditions. Case 2 proved the problem was indeed singular.

Case 3 drove a spacecraft which was spiralling out from Earth to rest at L_2 . Case 4 showed that the linearized dynamics were valid for Case 3. Therefore, the optimal control law successfully caused the spacecraft to be captured by the Moon.

II. Theory

In order for a spacecraft to be captured by a celestial body, it must enter the region of phase space where the gravity field of the target body is dominant. In the simplest case, there are two celestial bodies (primaries) and the spacecraft; the three body problem. With one celestial body and a spacecraft, the celestial body's gravity field dominates all of the phase space. Hence, the three body problem is the simplest nontrivial capture problem. Fortunately, the restricted three body problem adequately describes most capture scenarios in our solar system.

The solution to the problem of how to optimally cause a low thrust vehicle to be captured involves developing equations of motion, analysis of the motion, determination of the optimal control law, and solution of the two point boundary value problem.

The Restricted Three Body Problem

This study will be confined to the restricted three body problem. The restricted three body problem consists of two bodies revolving about their center of mass in a circular orbit at a distance l from each other. A third body of negligible mass, moves in the plane defined by the

two primaries. Since the third body is of negligible mass, it does not affect the motion of the primaries. The masses are considered to be point masses. The restricted problem of three bodies is to describe the motion of the third body. (4:8)

Since the primaries revolve in a circular orbit about the mass center, a rotating coordinate frame (xy) centered at the center of mass and rotating with constant angular velocity Ω , (shown in Fig. 1.), is introduced. The rotating frame is found by a rotation through the angle Ωt about the z -axis from the inertial XY frame.

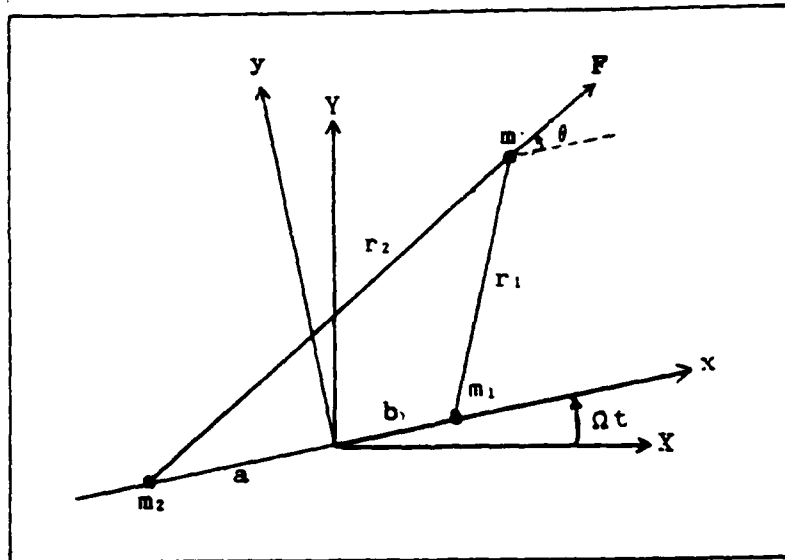


Fig. 1. Coordinate System for Restricted Three Body Problem

The position vector of the third body expressed in the rotating frame is

$$\mathbf{r} = x\hat{\mathbf{i}} + y\hat{\mathbf{j}} \quad (1)$$

where $\hat{\mathbf{i}}$ is a unit vector in the x direction

$\hat{\mathbf{j}}$ is a unit vector in the y direction.

The velocity is found by applying Coriolis' theorem for taking derivatives in a rotating frame, which is

$$\mathbf{v} = \left. \frac{d\mathbf{r}}{dt} \right|_I = \left. \frac{d\mathbf{r}}{dt} \right|_R + \boldsymbol{\omega} \times \mathbf{r} \quad (2)$$

where

$\left. \frac{d\mathbf{r}}{dt} \right|_I$ is the inertial time derivative

$\left. \frac{d\mathbf{r}}{dt} \right|_R$ is the time derivative in the rotating frame

$\boldsymbol{\omega}$ is the angular velocity of the rotating frame.

Performing the cross product produces

$$\mathbf{v} = (\dot{x} - \Omega y)\hat{\mathbf{i}} + (\dot{y} + \Omega x)\hat{\mathbf{j}} \quad (3)$$

Therefore, the kinetic energy of the third body is

$$T = \frac{1}{2}m(\mathbf{v} \cdot \mathbf{v}) = \frac{1}{2}m[(\dot{x} - \Omega y)^2 + (\dot{y} + \Omega x)^2] \quad (4)$$

The mass of the third body plays no role in the motion, hence the kinetic energy per unit mass becomes

$$T/m = \frac{1}{2}[(\dot{x} - \Omega y)^2 + (\dot{y} + \Omega x)^2] \quad (5)$$

The coordinates x and y may be nondimensionalized such that the new coordinates x and y equal the old x and y divided by the distance between the primaries, $l = a + b$, hence

$$T/ml^2 = \frac{1}{2}[(\dot{x} - \Omega y)^2 + (\dot{y} + \Omega x)^2] \quad (6)$$

Time is nondimensionalized by $dt^* = \Omega dt$, where t^* is the nondimensional time. Therefore,

$$\frac{dx}{dt} = \Omega \frac{dx}{dt^*}$$

Denoting $\dot{x} = dx/dt^*$ and $\dot{y} = dy/dt^*$, produces

$$T/ml^2 = \frac{1}{2}\Omega^2(\dot{x}^2 - 2\dot{x}\dot{y} + \dot{y}^2 + x^2 + y^2)$$

Kinetic energy is nondimensionalized by dividing by Ω^2 to yield

$$T^* = T/ml^2\Omega^2 = \frac{1}{2}(\dot{x}^2 + \dot{y}^2) + 2(x\dot{y} - \dot{x}y) + (x^2 + y^2) \quad (7)$$

The potential energy of the third body is the sum of the classical gravitational potentials due to the two primaries, so the potential energy expressed in dimensional coordinates is

$$V = -Gm(m_1/r_1 + m_2/r_2) \quad (8)$$

where

G is the universal gravity constant

m_1 and m_2 are the masses of the primaries

and

$$r_1 = [(x - b)^2 + y^2]^{\frac{1}{2}} \quad (9)$$

$$r_2 = [(x + a)^2 + y^2]^{\frac{1}{2}} \quad (10)$$

The potential energy per unit mass is given by

$$V/m = -G(m_1/r_1 + m_2/r_2) \quad (11)$$

Balance between gravitational and centrifugal forces requires:

$$Gm_1m_2/l^2 = m_2a\Omega^2 = m_1b\Omega^2 \quad (12)$$

hence

$$Gm_1 = a\Omega^2 l^2 \quad (13)$$

$$Gm_2 = b\Omega^2 l^2 \quad (14)$$

$$G(m_1 + m_2) = \Omega^2 l^2 \quad (15)$$

Two mass parameters, μ_1 and μ_2 are defined as follows:

$$\mu_1 = \frac{m_1}{m_1 + m_2}$$

$$\mu_2 = \frac{m_2}{m_1 + m_2}$$

and since the coordinate frame is centered at the center of mass of m_1 and m_2 , μ_1 and μ_2 become

$$\mu_1 = a/l \quad (16)$$

$$\mu_2 = b/l \quad (17)$$

Substituting (13) and (14) into (11) leads to

$$V/m = -(a\Omega^2 l^2/r_1 + b\Omega^2 l^2/r_2) \quad (18)$$

Dividing by Ω^2 yields

$$V/m\Omega^2 = -(al^2/r_1 + bl^2/r_2) \quad (19)$$

Now r_1 and r_2 are nondimensionalized by dividing by l .

Then substituting (16) and (17) into (9) and (10), the nondimensional r_1 and r_2 become

$$r_1 = [(x - \mu_2)^2 + y^2]^{\frac{1}{2}} \quad (20)$$

$$r_2 = [(x + \mu_1)^2 + y^2]^{\frac{1}{2}} \quad (21)$$

and therefore (19) becomes

$$V/m\Omega^2 = -(a/r_1 + b/r_2)$$

Substituting for a and b from (16) and (17) and dividing by l^2 yields the nondimensional form of the potential:

$$v^* = v/m\Omega^2 l^2 = -(\mu_1/r_1 + \mu_2/r_2) \quad (22)$$

Hamilton's equations are now used to derive four first order equations of motion from the expressions for kinetic and potential energy. Two new coordinates are introduced, called conjugate momenta, denoted p_x and p_y . Since the potential is not explicitly dependent on the rates \dot{x} and \dot{y} , the conjugate momenta may be found by

$$p_x = \partial T^* / \partial \dot{x}$$

$$p_y = \partial T^* / \partial \dot{y}$$

Taking the partials, p_x and p_y become

$$p_x = \dot{x} - y \quad (23)$$

$$p_y = \dot{y} + x \quad (24)$$

The kinetic energy is separated into terms which involve the rates, \dot{x} and \dot{y} , quadratically, linearly, and those terms which do not involve the rates; T^*_2 , T^*_1 , and T^*_0 respectively. The Hamiltonian is

$$H = T^*_2 + V^* - T^*_0$$

which yields

$$H = \frac{1}{2}(\dot{x}^2 + \dot{y}^2) - (\mu_1/r_1 + \mu_2/r_2) - \frac{1}{2}(x^2 + y^2) \quad (25)$$

Substituting for \dot{x} and \dot{y} using (23) and (24) leads to

$$H = \frac{1}{2}(p_x^2 + 2p_x y + p_y^2 - 2p_y x) - (\mu_1/r_1 + \mu_2/r_2) \quad (26)$$

If the only force acting is gravity, Hamilton's equations for this system are

$$\begin{aligned}\dot{x} &= \partial H / \partial p_x & \dot{y} &= \partial H / \partial p_y \\ \dot{p}_x &= -\partial H / \partial x & \dot{p}_y &= -\partial H / \partial y\end{aligned}\quad (27)$$

The thrust vector applied to the spacecraft is defined as follows:

$$\mathbf{F} = F \cos\theta \hat{i} + F \sin\theta \hat{j} \quad (28)$$

where F is a nondimensional constant thrust magnitude, ($F = \text{thrust}/mI\Omega^2$), and θ is the angle of the thrust vector relative to the local horizontal. This is a force which is not accounted for in the potential, so Hamilton's equations become

$$\begin{aligned}\dot{x} &= \partial H / \partial p_x & \dot{y} &= \partial H / \partial p_y \\ \dot{p}_x &= -\partial H / \partial x + Q_x & \dot{p}_y &= -\partial H / \partial y + Q_y\end{aligned}\quad (29)$$

where

$$Q_x = \mathbf{F} \cdot \partial \mathbf{v} / \partial \dot{x} \quad Q_y = \mathbf{F} \cdot \partial \mathbf{v} / \partial \dot{y}$$

which yields

$$Q_x = F \cos\theta \quad Q_y = F \sin\theta \quad (30)$$

Substituting (30) into Hamilton's equations and taking the indicated derivatives of H , the equations of motion become

$$\begin{aligned}\dot{x} &= p_x + y & (31) \\ \dot{y} &= p_y - x \\ \dot{p}_x &= p_y - [\mu_1(x - \mu_2)/r_1^3 + \mu_2(x + \mu_1)/r_2^3] + F \cos\theta \\ \dot{p}_y &= -p_x - y[\mu_1/r_1^3 + \mu_2/r_2^3] + F \sin\theta\end{aligned}$$

Note that μ_1 and μ_2 may be between 0 and 1 and $\mu_2 = 1 - \mu_1$, so these two parameters may be consolidated.

Let $\mu = \mu_2$, then $\mu_1 = 1 - \mu$, which leads to the equations of motion:

$$\dot{x} = p_x + y \quad (32)$$

$$\dot{y} = p_y - x$$

$$\dot{p}_x = p_y - [(1-\mu)(x - \mu)/r_1^3 + \mu(x + (1-\mu))/r_2^3] + F \cos\theta$$

$$\dot{p}_y = -p_x - y[(1-\mu)/r_1^3 + \mu/r_2^3] + F \sin\theta$$

where

$$r_1 = [(x - \mu)^2 + y^2]^{\frac{1}{2}}$$

$$r_2 = [(x + (1-\mu))^2 + y^2]^{\frac{1}{2}}$$

Regions of Motion and Capture Criterion

The equations of motion for a thrusting spacecraft in the restricted three body problem are shown in eqn. (32). Unforced motion in the restricted three body problem has been studied since 1772. (4:4) Analysis of this motion will help determine a definition of capture and a performance index for an optimal control law.

For the unforced motion, all forces are accounted for in the Lagrangian. Since the Hamiltonian is not an explicit function of time, $\dot{H} = \partial H / \partial t = 0$, it is an integral of the motion, called the Jacobi integral. The introduction of this integral was Jacobi's major contribution to this problem in 1836. (4:4) Since $\dot{H} = 0$, H is constant, therefore the motion must take place in such a

manner which renders the Hamiltonian constant over time. This leads to some deductions about the motion.

Recall

$$H = \frac{1}{2}(\dot{x}^2 + \dot{y}^2) - (\mu_1/r_1 + \mu_2/r_2) - \frac{1}{2}(x^2 + y^2)$$

which is constant over time. Therefore, setting $H = -C$ (a constant) and rearranging yields

$$\dot{x}^2 + \dot{y}^2 = 2(\mu_1/r_1 + \mu_2/r_2) + (x^2 + y^2) - 2C$$

which may be written

$$\dot{x}^2 + \dot{y}^2 = 2U(x,y) - 2C \quad (33)$$

The left hand side of (33) is always greater than zero, which implies motion only exists if $U(x,y) \geq C$. The equation $U(x,y) = C$ defines "curves of zero velocity."

Figs. 2 through 5 depict these curves for various μ . The constant C is determined by the initial conditions.

Setting $y = 0$ determines how the Hamiltonian or Jacobi integral varies along the x -axis for various values of μ (shown in Fig. 6). There are three local maxima along the x -axis. These are unstable equilibrium points called L_1 , L_2 , and L_3 , which are referred to as Lagrange points.

(4:142)

Curves of zero velocity provide information about the possible motion in regions of the x - y plane. In order to be captured by a celestial body, a spacecraft must enter the region of phase space where the motion consists of a closed orbit about that body. It is difficult to visualize a four

dimensional phase space, however, the curves of zero velocity characterize the motion in terms of the two position coordinates and the Jacobi integral (which is a measure of energy).

The region of the phase space which defines capture is bounded by the contour of the zero velocity curve passing through L_2 because if the spacecraft is in this region of the x-y plane with a value of the Jacobi integral less than that of the contour passing through L_2 , the spacecraft cannot leave this region. This is the definition of capture.

The question now becomes: what direction should the thrust be applied to optimally cause the spacecraft which is captured by one body to be captured by the other? The two capture regions touch at L_2 . L_2 is a saddle point because the Jacobi integral has a local maximum at L_2 along the x direction, but has a local minimum along the y direction there. To enter the target capture region at any point other than L_2 requires a Jacobi integral (and hence energy) greater than that of the zero velocity curve passing through L_2 because the spacecraft must leave the initial capture region. Therefore, this is the point where a spacecraft captured by one body may be caused to be captured by the other by adding the least energy.

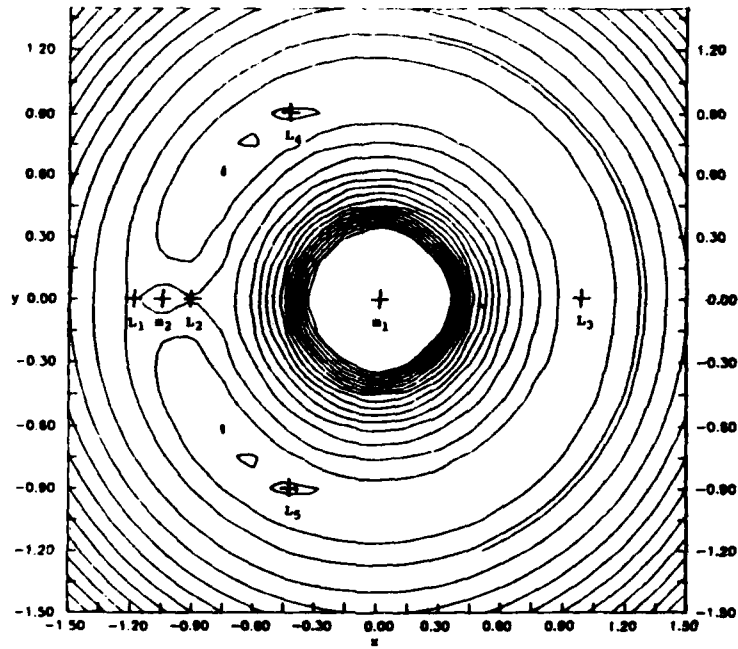


Fig. 2. Curves of Zero Velocity for $\mu = 0.01$

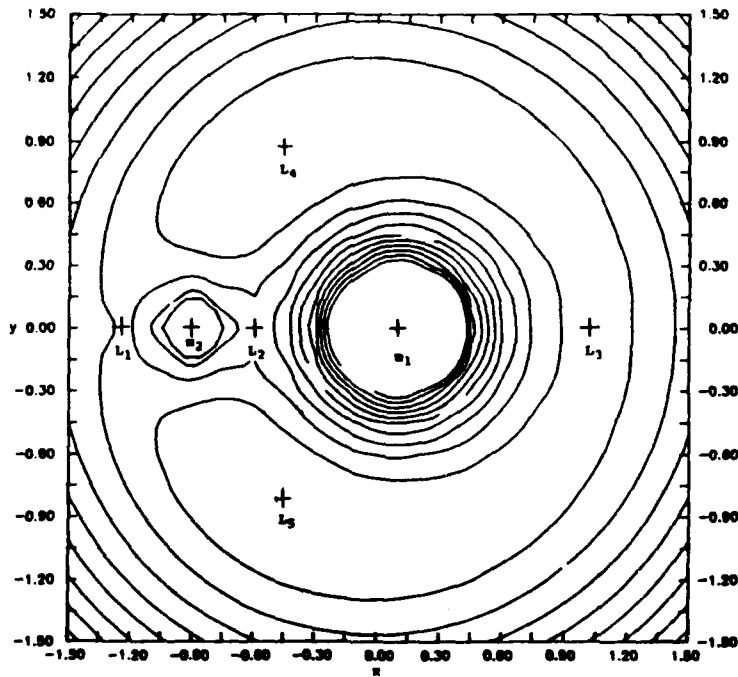


Fig. 3. Curves of Zero Velocity for $\mu = 0.1$

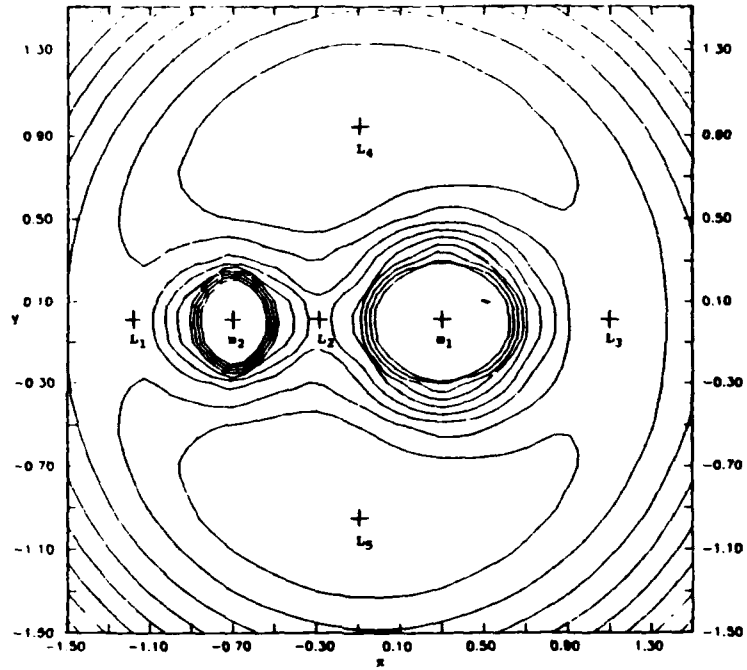


Fig. 4. Curves of Zero Velocity for $\mu = 0.3$

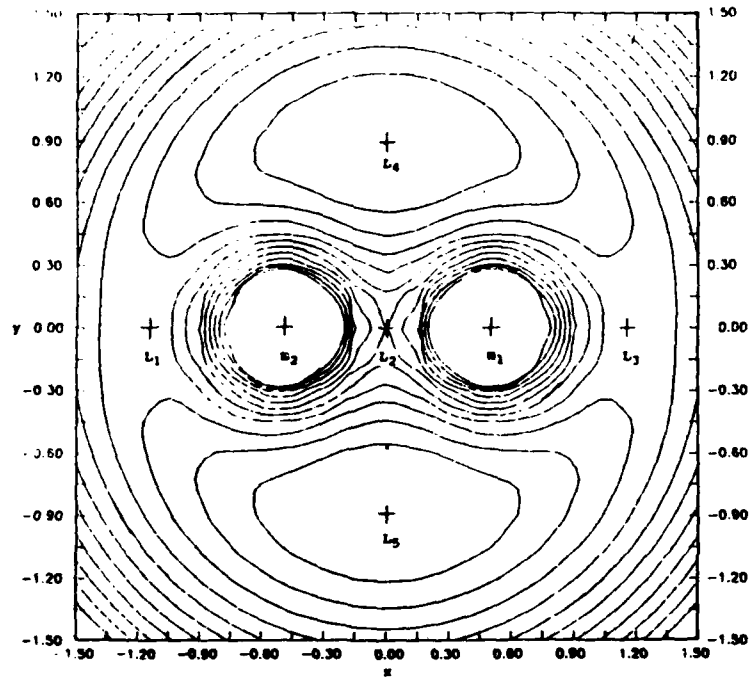


Fig. 5. Curves of Zero Velocity for $\mu = 0.5$

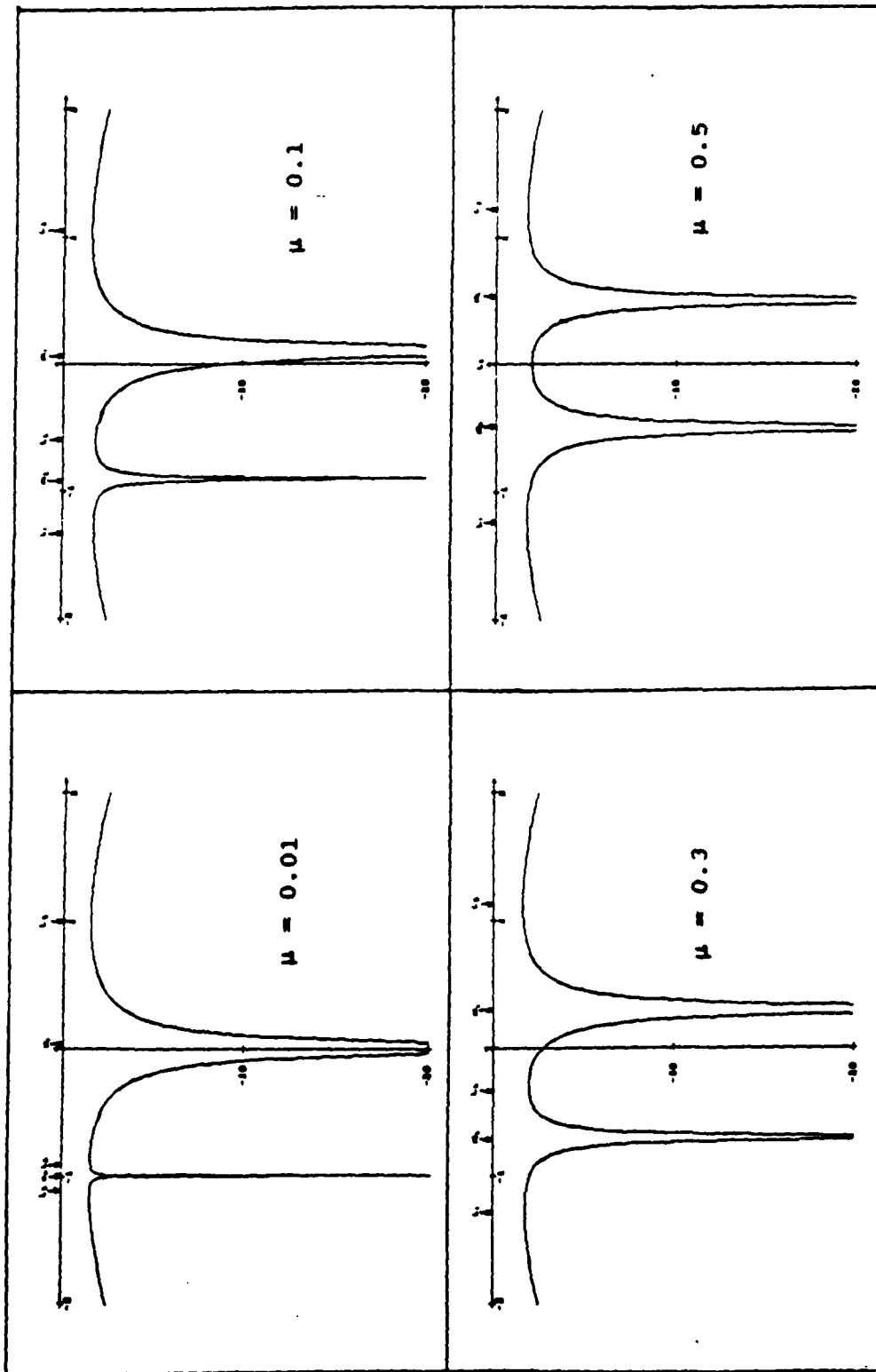


Fig. 6. The Jacobi Integral along the X-axis for various μ

The Optimal Control Law

The general optimal control problem is to determine the control which will drive a system to a desired set of final conditions, while minimizing a cost function or performance index. This cost function is usually expressed in the form of an integral

$$PI = \int_{t_i}^{t_f} L(x, u, t) dt$$

where x is the state vector and u is the control vector.

The Jacobi integral suggests itself as a logical choice for a performance index because the Jacobi integral must be increased to cause capture. A large difficulty with optimal control theory is choosing a proper performance index since a system may behave optimally for the given performance index, there is no guarantee the given performance index is really "optimal." Therefore, performance indices with physical significance usually are preferred. In this case, the Jacobi integral or Hamiltonian has a definite physical significance.

The control variable for this problem is θ . Constant thrust will be assumed to be applied to a spacecraft of constant mass. Since the thrust magnitude is constant, the problem is to determine the function $\theta(t)$ which will drive the system to be captured as quickly as possible.

The equations of motion have been developed, a performance index chosen, and desired final conditions determined. The calculus of variations is used to determine necessary conditions to minimize the performance index. In order to drive the spacecraft toward L_2 from the vicinity of one of the bodies, the Jacobi integral must be increased. Thus if $-\dot{H}$ is minimized, increase in H will be maximized, driving the spacecraft toward capture. This performance index expressed in integral form becomes

$$PI = \int_{t_i}^{t_f} -\dot{H} dt$$

Since the system is constrained to obey the equations of motion, Lagrange multipliers (costates) are introduced so the performance index becomes

$$PI = \int_{t_i}^{t_f} (-\dot{H} + \lambda^T f) dt$$

where λ is a vector of costates and the elements of f are the equations of motion in vector form.

The chain rule is used to determine \dot{H} , which is

$$\dot{H} = \dot{x} \partial H / \partial x + \dot{y} \partial H / \partial y + \dot{p}_x \partial H / \partial p_x + \dot{p}_y \partial H / \partial p_y$$

The partial derivatives are found by using Hamilton's equations (29) so that \dot{H} becomes

$$\dot{H} = (F \cos \theta - \dot{p}_x) \dot{x} + (F \sin \theta - \dot{p}_y) \dot{y} + \dot{x} \dot{p}_x + \dot{y} \dot{p}_y$$

which simplifies to

$$H = \dot{x} F \cos \theta + \dot{y} F \sin \theta \quad (34)$$

The necessary conditions for a minimum are found by taking the first variation of PI, integrating by parts, and setting that equal to zero, which produces the Euler equation and boundary conditions. This is presented by Schultz and Melsa for a general PI. (3:233-249) Those results will be employed to determine the optimal control law. The state function of Pontryagin (also known as the control Hamiltonian) is

$$H_C = -\dot{H} + \lambda^T f(x, \theta, t)$$

where the equations of motion are

$$\dot{x} = f(x, \theta, t)$$

and

$$x = (x \ y \ p_x \ p_y)^T$$

and λ is a vector of four Lagrange multipliers or costates. Substituting for \dot{H} and f , the control Hamiltonian becomes

$$\begin{aligned} H_C = & -\dot{x}F \cos\theta - \dot{y}F \sin\theta + \lambda_1(p_x + y) + \lambda_2(p_y - x) + \\ & \lambda_3\{p_y - [(1-\mu)(x - \mu)/r_1^3 + \mu(x + (1-\mu))/r_2^3] + F \cos\theta\} \\ & + \lambda_4\{-p_x - y[(1-\mu)/r_1^3 + \mu/r_2^3] + F \sin\theta\} \quad (35) \end{aligned}$$

The optimal control is found by setting $\partial H_C / \partial \theta = 0$, which yields

$$\partial H_C / \partial \theta = \dot{x}F \sin\theta - \dot{y}F \cos\theta - \lambda_3 F \sin\theta + \lambda_4 F \cos\theta = 0$$

Dividing through by F and grouping $\sin\theta$ and $\cos\theta$ leads to

$$(\dot{x} - \lambda_3)\sin\theta + (\lambda_4 - \dot{y})\cos\theta = 0$$

Hence, the optimal control law is

$$\tan \theta = \frac{(\dot{y} - \lambda_4)}{(\dot{x} - \lambda_3)} \quad (36)$$

and therefore the optimal thrust angle θ^* is

$$\theta^* = \tan^{-1}[(\dot{y} - \lambda_4)/(\dot{x} - \lambda_3)] \quad (37)$$

The sine and cosine of the optimal thrust angle are

$$\sin \theta^* = \frac{\dot{y} - \lambda_4}{[(\dot{y} - \lambda_4)^2 + (\dot{x} - \lambda_3)^2]^{\frac{1}{2}}} \quad (38)$$

$$\cos \theta^* = \frac{\dot{x} - \lambda_3}{[(\dot{y} - \lambda_4)^2 + (\dot{x} - \lambda_3)^2]^{\frac{1}{2}}}$$

Substituting for \dot{x} and \dot{y} from (32) produces

$$\sin \theta^* = \frac{p_y - x - \lambda_4}{[(p_y - x - \lambda_4)^2 + (p_x + y - \lambda_3)^2]^{\frac{1}{2}}} \quad (39)$$

$$\cos \theta^* = \frac{p_x + y - \lambda_3}{[(p_y - x - \lambda_4)^2 + (p_x + y - \lambda_3)^2]^{\frac{1}{2}}}$$

The optimal trajectory will obey the following:

$$\dot{\mathbf{x}} = \partial H_C / \partial \lambda \quad \dot{\lambda} = -\partial H_C / \partial \mathbf{x}$$

The first four equations, $\dot{\mathbf{x}} = \partial H_C / \partial \lambda$, are the equations of motion (32) with the optimal thrust angle θ^* substituted for θ . The remaining four equations, which describe how the costates vary in time, are as follows:

$$\dot{\lambda}_1 = -F \sin \theta^* + \lambda_2 + \frac{\lambda_3(1 - \mu)}{r_1^3} + \frac{\mu \lambda_3}{r_2^3} - \frac{3(1 - \mu)(x - \mu)[\lambda_3(x - \mu) + \lambda_4 y]}{r_1^5}$$

$$- \frac{3\mu[x + (1 - \mu)]\{\lambda_3[x + (1 - \mu)] + \lambda_4 y\}}{r_2^5} \quad (40)$$

$$\dot{\lambda}_2 = F \cos\theta^* - \lambda_1 + \frac{\lambda_4(1 - \mu)}{r_1^3} + \frac{\mu\lambda_4}{r_2^3} - \frac{3y(1 - \mu)[\lambda_3(x - \mu) + \lambda_4 y]}{r_1} - \frac{3\mu y\{\lambda_3[x + (1 - \mu)] + \lambda_4 y\}}{r_2^5} \quad (41)$$

$$\dot{\lambda}_3 = F \cos\theta^* - \lambda_1 + \lambda_4 \quad (42)$$

$$\dot{\lambda}_4 = F \sin\theta^* - \lambda_2 - \lambda_3 \quad (43)$$

The second derivative of H_C with respect to θ must be greater than 0 to insure a local minimum. (2:184).

Therefore, for a local minimum

$$\partial^2 H_C / \partial \theta^2 = (\dot{x} - \lambda_3) \cos\theta - (\lambda_4 - \dot{y}) \sin\theta > 0 \quad (44)$$

Along a stationary trajectory, $\cos\theta$ and $\sin\theta$ are given by (38), which leads to

$$\frac{(\dot{x} - \lambda_3)^2 + (\dot{y} - \lambda_4)^2}{[(p_y - x - \lambda_4)^2 + (p_x + y - \lambda_3)^2]^{\frac{1}{2}}} > 0 \quad (45)$$

which is satisfied because the positive square root is chosen by the definition of the sine and cosine, so along any stationary path, a local minimum is guaranteed.

Two Point Boundary Value Problem

Since the equations of motion and optimal control law have been developed, solving the boundary value problem is next step. Unfortunately, boundary conditions are determined at both the initial and final times. At the initial time, t_i , the four states are known but the costates are not. Also, at the final time, t_f , the desired states are determined and the costates are undetermined.

Taking the first variation of the performance index, PI, and integrating by parts from t_i to t_f yields the following boundary condition:

$$-\lambda_1 dx - \lambda_2 dy - \lambda_3 dp_x - \lambda_4 dp_y + H_C dt = 0 \quad (46)$$

evaluated at t_f . Since the states at t_f are fixed,

$$dx = dy = dp_x = dp_y = 0$$

so $H_C dt = 0$. If t_f is specified, $dt = 0$ so the boundary conditions are satisfied. If t_f is not specified, t_f is chosen so that $H_C = 0$ at t_f . This value of t_f minimizes PI.

The problem is to determine the initial costates to drive the system to rest at L_2 . No closed form solution to this problem is known since no closed form solution to the restricted three body problem is known and a nonlinear control is being applied, therefore a numerical solution is called for. The shooting method was chosen to solve this problem.

The shooting method is derived from the behavior of linearized dynamics. The equations of motion form a set of eight nonlinear ordinary differential equations which is expressed in vector form as

$$\dot{\mathbf{X}} = \mathbf{g}(\mathbf{X}, t) \quad (47)$$

Expanding about a desired trajectory, \mathbf{X}_0 , in a Taylor series by letting $\mathbf{X} = \mathbf{X}_0 + \delta\mathbf{X}$ and substituting into the equations of motion produces

$$\dot{\mathbf{X}} = \frac{d(\mathbf{X}_0 + \delta\mathbf{X})}{dt} = \mathbf{g}(\mathbf{X}_0 + \delta\mathbf{X}, t) \quad (48)$$

$$\frac{d\mathbf{X}_0}{dt} + \frac{d\delta\mathbf{X}}{dt} = \mathbf{g}(\mathbf{X}_0, t) + \nabla_{\mathbf{X}}\mathbf{g}(\mathbf{X}_0, t)\delta\mathbf{X} + O(2) \quad (49)$$

Cancelling the equations of motion for the desired trajectory, yields the equations of variation:

$$\dot{\delta\mathbf{X}} = \mathbf{A}(t)\delta\mathbf{X} \quad (50)$$

where $\mathbf{A}(t) = \nabla_{\mathbf{X}}\mathbf{g}(\mathbf{X}_0, t)$, which is evaluated along the time dependent desired trajectory. The equations of variation are linear ordinary differential equations, so a set of independent solutions ϕ_i may be constructed as follows:

$$\dot{\phi}_i = \mathbf{A}(t)\phi_i ; \phi_{ij}(t_i) = \delta_{ij} \quad (51)$$

where δ_{ij} is the Kroenecker delta. Any solution to the equations of variation may be written

$$\delta\mathbf{X}(t) = \sum \delta\mathbf{X}_i(t_i)\phi_i(t)$$

where $\delta\mathbf{X}_i(t_i)$ are the components of $\delta\mathbf{X}$ at t_i . The ϕ_i form

a fundamental set of solutions, so assembling the vector columns of ϕ_i into a matrix ϕ leads to the expression:

$$\delta X(t) = \phi(t, t_i) \delta X(t_i) \quad (52)$$

The state transition matrix, ϕ satisfies

$$\dot{\phi} = A(t)\phi ; \phi(t_i, t_i) = I \quad (53)$$

where I is the identity matrix. This equation, along with the equations of motion are numerically integrated from t_i to t_f . (5:24-27)

Applying this to the case at hand, X is defined as

$$X = \begin{Bmatrix} x \\ \lambda \end{Bmatrix}$$

Eqn. (52) is partitioned as follows:

$$\begin{Bmatrix} \delta x(t_f) \\ \delta \lambda(t_f) \end{Bmatrix} = \begin{bmatrix} \phi_{xx} & | & \phi_{x\lambda} \\ \hline \phi_{\lambda x} & | & \phi_{\lambda\lambda} \end{bmatrix} \begin{Bmatrix} \delta x(t_i) \\ \delta \lambda(t_i) \end{Bmatrix} \quad (54)$$

Hence, the variation in the final states due to small changes in initial conditions may be written:

$$\delta x(t_f) = \phi_{xx} \delta x(t_i) + \phi_{x\lambda} \delta \lambda(t_i) \quad (55)$$

but since $x(t_i)$ is fixed, $\delta x(t_i) = (0)$ so

$$\delta x(t_f) = \phi_{x\lambda} \delta \lambda(t_i) \quad (56)$$

Eqn. (56) is an expression which determines how to change $\lambda(t_i)$ to obtain a desired change in $x(t_f)$. Solving for $\delta \lambda(t_i)$, produces

$$\delta \lambda(t_i) = \phi_{x\lambda}^{-1} \delta x(t_f) \quad (57)$$

The shooting method starts by estimating a set of initial costates and integrating the equations of motion

and the equation for $\dot{\lambda}$, (53), from t_i to t_f . This produces $x(t_f)$ for the first iteration. $\delta x(t_f)$ is the difference between $x(t_f)$ and the desired $x(t_f)$. Then equation (57) determines the correction to the initial costates. The next set of initial costates will be the previous initial costates minus $\delta \lambda(t_i)$, and the process is repeated until a trajectory from $x(t_i)$ to the desired $x(t_f)$ is found.

III. Results and Discussion

The first practical application of this theory will be in the Earth-Moon system. This case has the highest value of μ for any three body problem in the solar system. At this point attention is confined to the Earth-Moon case for fixed final times. For the Earth-Moon system:

$$\Omega = 2.649 \times 10^{-6} \text{ radians/sec (1:337)}$$

$$l = 384,400 \text{ km. (1:323)}$$

$$\mu = 0.0121506683$$

and L_2 is located at $x_{L_2} = -0.8369147190$ along the x-axis.
(4:221)

The first step was to verify the equations of motion and the numerical integrator. The integration algorithm used was a routine called Haming, which is used in Mech. 731. (5) The equations of motion (eqns. (32), (38), (40)-(43)) were programmed and then tested. There is a periodic orbit which alternates between the earth and the moon found by Davidson in 1964 for $\mu = 1/81.45$ and no thrust. (4:509-510) This orbit was computed with initial conditions: $x = -1.15$, $y = 0.0$, $p_x = 0.0$, $p_y = -1.15868829$; with a step size of 1000 integration steps per time unit. This value of step size was chosen to insure that H remained constant. The orbit was successfully reproduced, (shown in Fig. 7), verifying the

numerical integration algorithm and the unforced equations of motion were correct.

In the Vicinity of L_2

Capture will occur when the spacecraft comes to rest at L_2 . Far away from L_2 , the effect of the third body is small, therefore the region near L_2 is of most interest. Since L_2 is an equilibrium point, the dynamics may be linearized around L_2 using (50). The elements of A may be defined as

$$A(t) = \begin{bmatrix} a_{11} & a_{12} & a_{13} & a_{14} \\ a_{21} & a_{22} & a_{23} & a_{24} \\ a_{31} & a_{32} & a_{33} & a_{34} \\ a_{41} & a_{42} & a_{43} & a_{44} \end{bmatrix} = \nabla_{\mathbf{x}} f(\mathbf{x}, t) |_{L_2} \quad (58)$$

then the nontrivial partials are

$$a_{31} = -\frac{(1-\mu)}{r_1^3} + \frac{3(1-\mu)(x-\mu)^2}{r_1^5} - \frac{\mu}{r_2^3} + \frac{3\mu(x+(1-\mu))^2}{r_2^5} \quad (59)$$

$$a_{32} = \frac{3(1-\mu)y}{r_1^5} + \frac{3\mu(x+(1-\mu))y}{r_2^5}$$

$$a_{41} = \frac{3y(1-\mu)(x-\mu)}{r_1^5} + \frac{3y\mu(x+(1-\mu))}{r_2^5}$$

$$a_{42} = -\frac{(1-\mu)}{r_1^3} + \frac{3y^2(1-\mu)}{r_1^5} - \frac{\mu}{r_2^3} + \frac{3\mu y^2}{r_2^5}$$

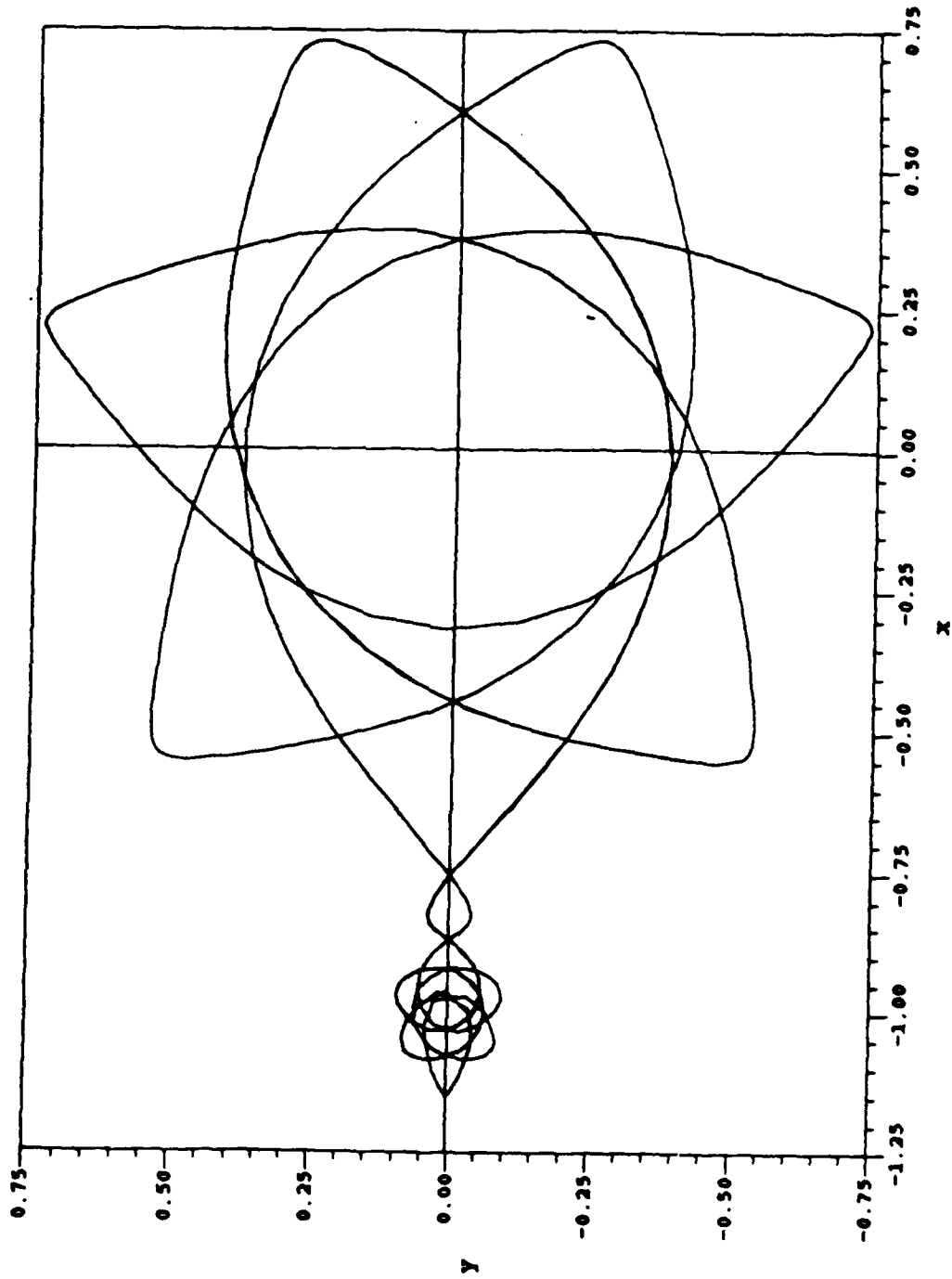


Fig. 7. Periodic Orbit in Earth/Moon System

Evaluating at L_2 ; $x = x_{L_2}$, $y = 0$, $\dot{x} = 0$, $\dot{y} = 0$, leads to

$$A(t) = \begin{bmatrix} 0 & 1 & 1 & 0 \\ -1 & 0 & 0 & 1 \\ a_{31} & 0 & 0 & 1 \\ 0 & a_{42} & -1 & 0 \end{bmatrix}$$

where

$$a_{31} = 10.29519541$$

$$a_{42} = -5.147597707$$

A new set of variables are defined as follows:

$$X = \begin{Bmatrix} x_1 \\ x_2 \\ x_3 \\ x_4 \end{Bmatrix} = \begin{Bmatrix} x - x_{L_2} \\ y \\ p_x \\ p_y - x_{L_2} \end{Bmatrix} \quad (60)$$

Therefore, the equations of motion near L_2 with thrust applied become

$$\dot{x}_1 = x_2 + x_3 \quad (61)$$

$$\dot{x}_2 = -x_1 + x_4$$

$$\dot{x}_3 = a_{31}x_1 + x_4 + F\cos\theta$$

$$\dot{x}_4 = a_{42}x_2 - x_3 + F\sin\theta$$

Using Hamilton's equations and the chain rule as in (34), \dot{H} becomes

$$\dot{H} = \dot{x}_1 F\cos\theta + \dot{x}_2 F\sin\theta \quad (62)$$

Substituting for \dot{x}_1 and \dot{x}_2 from (61) leads to

$$H = (x_2 + x_3)F\cos\theta + (-x_1 + x_4)F\sin\theta$$

The control Hamiltonian becomes

$$H_C = -\dot{H} + \lambda_1(x_2 + x_3) + \lambda_2(-x_1 + x_4) \\ + \lambda_3(a_{31}x_1 + x_4 + F\cos\theta) + \lambda_4(a_{42}x_2 - x_3 + F\sin\theta)$$

The optimal control law, $\partial H_C / \partial \theta = 0$, is

$$\tan\theta = \frac{(-x_1 + x_4 - \lambda_4)}{(x_2 + x_3 - \lambda_3)} \quad (63)$$

hence

$$\sin\theta = \frac{(-x_1 + x_4 - \lambda_4)}{[(x_2 + x_3 - \lambda_3)^2 + (-x_1 + x_4 - \lambda_4)^2]^{\frac{1}{2}}} \quad (64)$$

$$\cos\theta = \frac{(x_2 + x_3 - \lambda_3)}{[(x_2 + x_3 - \lambda_3)^2 + (-x_1 + x_4 - \lambda_4)^2]^{\frac{1}{2}}} \quad (65)$$

As before, the costates obey $\dot{\lambda} = -\partial H_C / \partial x$, where

$$\dot{\lambda}_1 = \lambda_2 - a_{31}\lambda_3 - F\sin\theta \quad (66)$$

$$\dot{\lambda}_2 = -\lambda_1 - a_{42}\lambda_4 + F\cos\theta$$

$$\dot{\lambda}_3 = -\lambda_1 + \lambda_4 + F\cos\theta$$

$$\dot{\lambda}_4 = -\lambda_2 - \lambda_3 + F\sin\theta$$

The state transition matrix, Φ , for this system is found by (53) where the matrix A in this case is the 8 by 8 Jacobian of the equations (61) and (66). The eight equations (61) and (66), along with the differential equation for Φ may be integrated from t_i to t_f . Then Φ may be verified by changing the initial conditions of the states and costates by a known amount. The change in the final conditions due to this change in initial conditions is predicted by (56). These predicted values were compared

to the actual changes in final conditions for several cases to verify Φ was computed correctly.

Next, the shooting method was implemented using equations using (61) and (66). However, eqn.(57) could not be solved because $\Phi_{x\lambda}$ was singular. When this occurs, changes may be made to the initial costates which cause no change in the final states. One solution to this problem is to not make changes to the initial costates along the eigenvector associated with the zero eigenvalue of $\Phi_{x\lambda}$.

Recalling (56), $\delta x(t_f) = \Phi_{x\lambda} \delta \lambda(t_i)$, $\Phi_{x\lambda}$ may be expressed

$$\Phi_{x\lambda} = EJE^{-1} \quad (67)$$

where E is the matrix of eigenvectors and J is a diagonal matrix with the eigenvalues: ξ_1, ξ_2, ξ_3 , and ξ_4 , on the diagonal, so therefore,

$$\delta x(t_f) = EJE^{-1} \delta \lambda(t_i) \quad (68)$$

Premultiplying by E^{-1} yields

$$E^{-1} \delta x(t_f) = JE^{-1} \delta \lambda(t_i) \quad (69)$$

The following vectors may be defined

$$q = E^{-1} \delta x(t_f)$$

$$s = E^{-1} \delta \lambda(t_i)$$

Therefore (69) is expressed

$$q = Js \quad (70)$$

which is an uncoupled set of equations:

$$q_i = \xi_i s_i \quad i = 1, \dots, 4 \quad (71)$$

Solving for s_i yields

$$s_i = q_i/\xi_i \quad (72)$$

Now if $\Phi_{x\lambda}$ is singular, at least one eigenvalue $\xi_j = 0$.

Since s_j is arbitrary, set $s_j = 0$. Solving for $\delta\lambda(t_i)$ produces

$$\delta\lambda(t_i) = Es \quad (73)$$

Since s_j is set to zero, no corrections are made to the initial costates along the null eigenvector.

Case 1

The purpose of Case 1 was to find any converging trajectory. The radius of convergence for the modified shooting method was found to be very small. In order to produce a converging trajectory, the initial states and the first estimate of the initial costates had to integrate to within about 10^{-3} of L_2 in position and 10^{-6} in velocity. This trajectory was found by integrating backwards from L_2 . For Case 1, $t_f = 0.7$ which is equal to 73.403 hours, and $F = 0.1$. The initial conditions for this case are as follows:

$$x_1 = 0.015865410$$

$$x_2 = 0.018917850$$

$$x_3 = -0.07711602$$

$$x_4 = -0.03304073$$

and the initial thrust angle is $\theta = 11.647$ degrees. The initial distance from L_2 is 9490.84 km. At the initial

conditions, the magnitude of gravity and Coriolis forces is 0.1318, so the thrust applied is less than gravity and Coriolis. Therefore this is a low thrust situation by the definition stated in the introduction. Fig. 8 shows x_1 vs x_2 and Fig. 9 shows the thrust angle θ vs time.

The eigenvector associated with the zero eigenvalue of $\Phi_{x\lambda}$ for this trajectory is

$$\xi = (1.0 \quad -0.12876 \quad 0.29116 \quad 0.060112)^T \quad (74)$$

The purpose of Case 2 was to verify that changes in the initial costates along this vector cause no change in the final states.

Case 2

This case used the same initial states, final time and thrust as Case 1. The initial costates were changed by 0.1 multiplied by (74). The trajectory for this case is shown in Fig. 10 and θ vs time is shown in Fig. 11. $\theta(t)$ for this case exactly matched $\theta(t)$ in Case 1 so the same control was applied despite different costates. Since the control applied was the same, the trajectory was exactly the same as Case 1. This confirms that changing the initial costates along the null eigenvector produced no change in the final states.

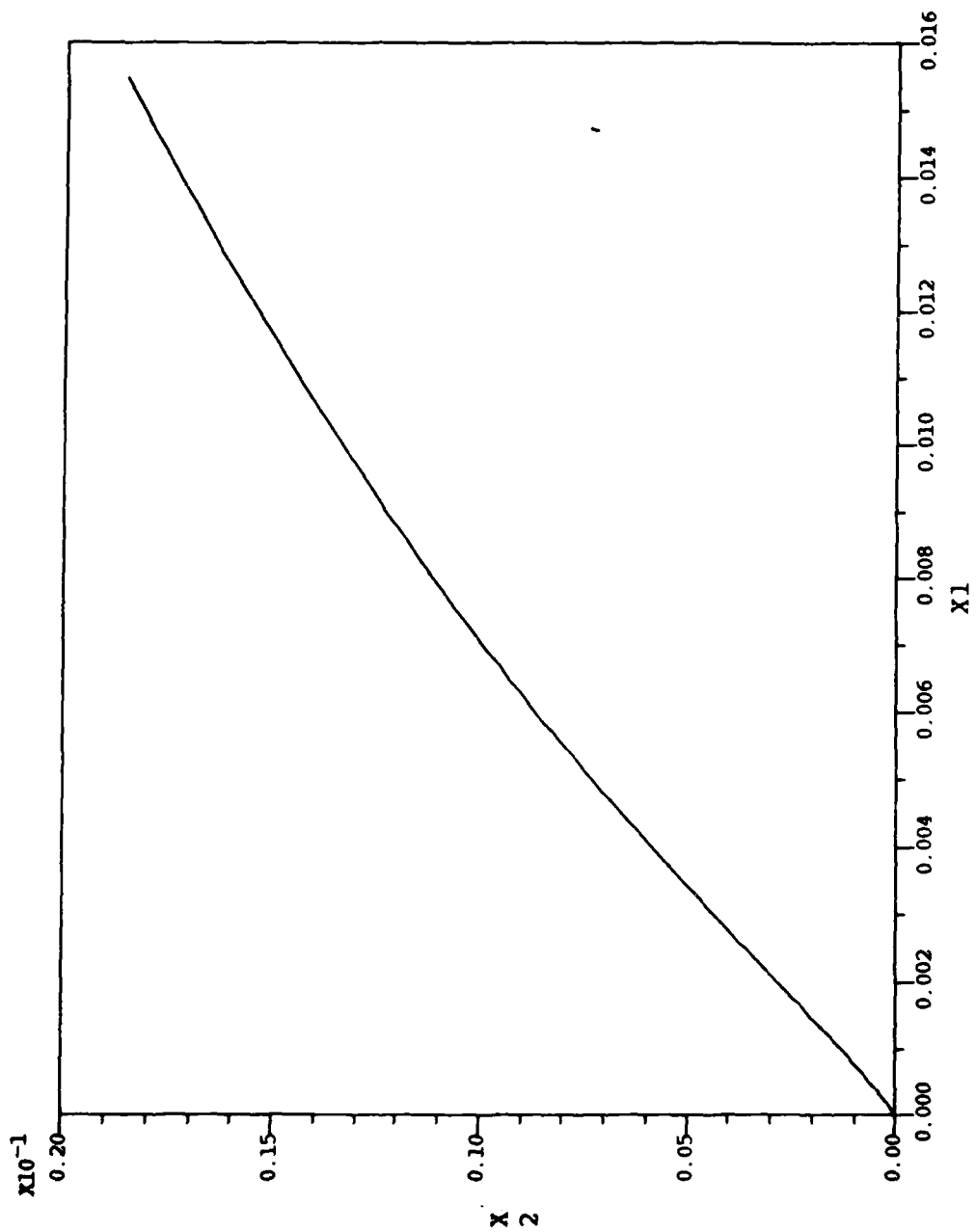


Fig. 8. Trajectory for Case 1

X
2

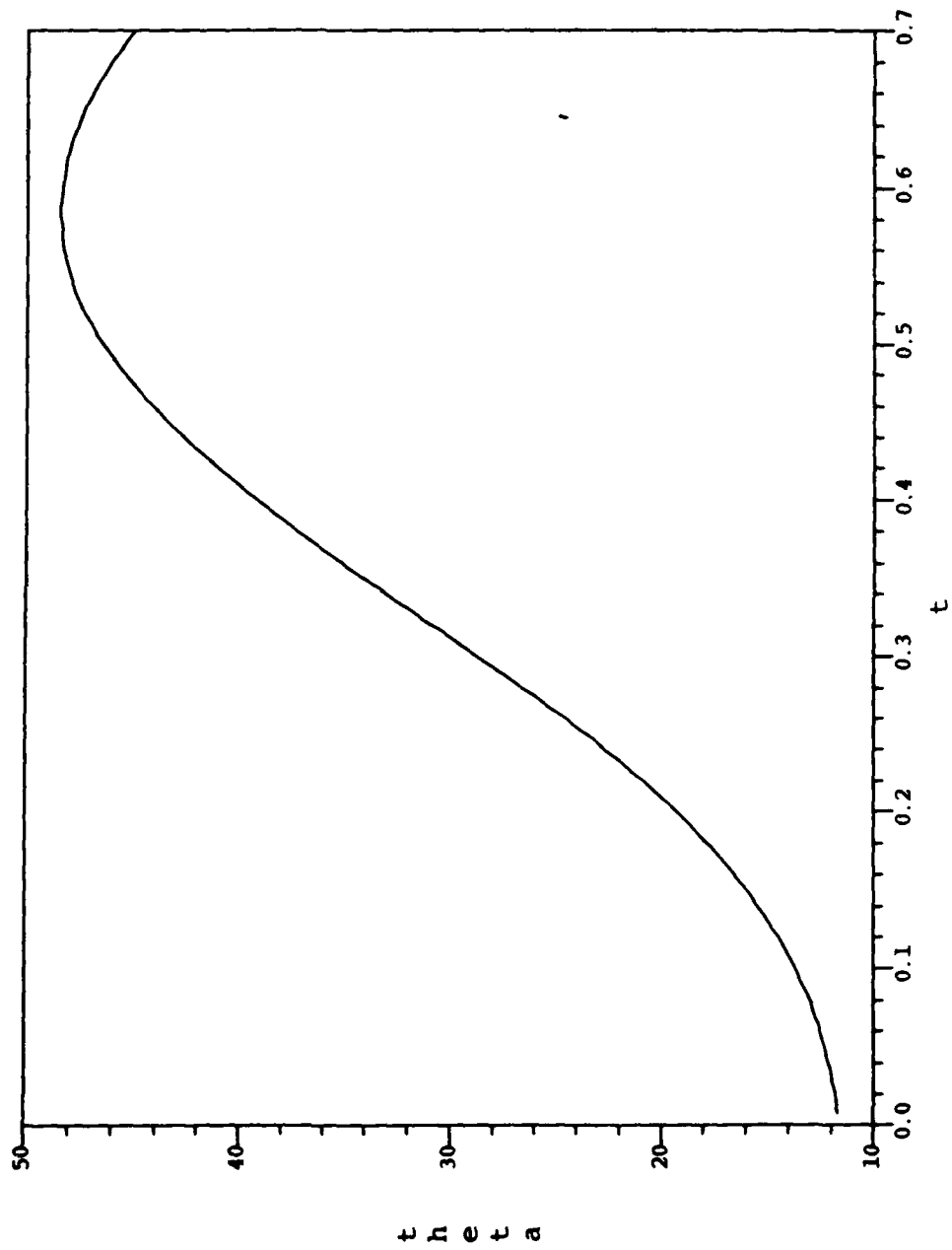


Fig. 9. Theta (degrees) vs Time for Case 1

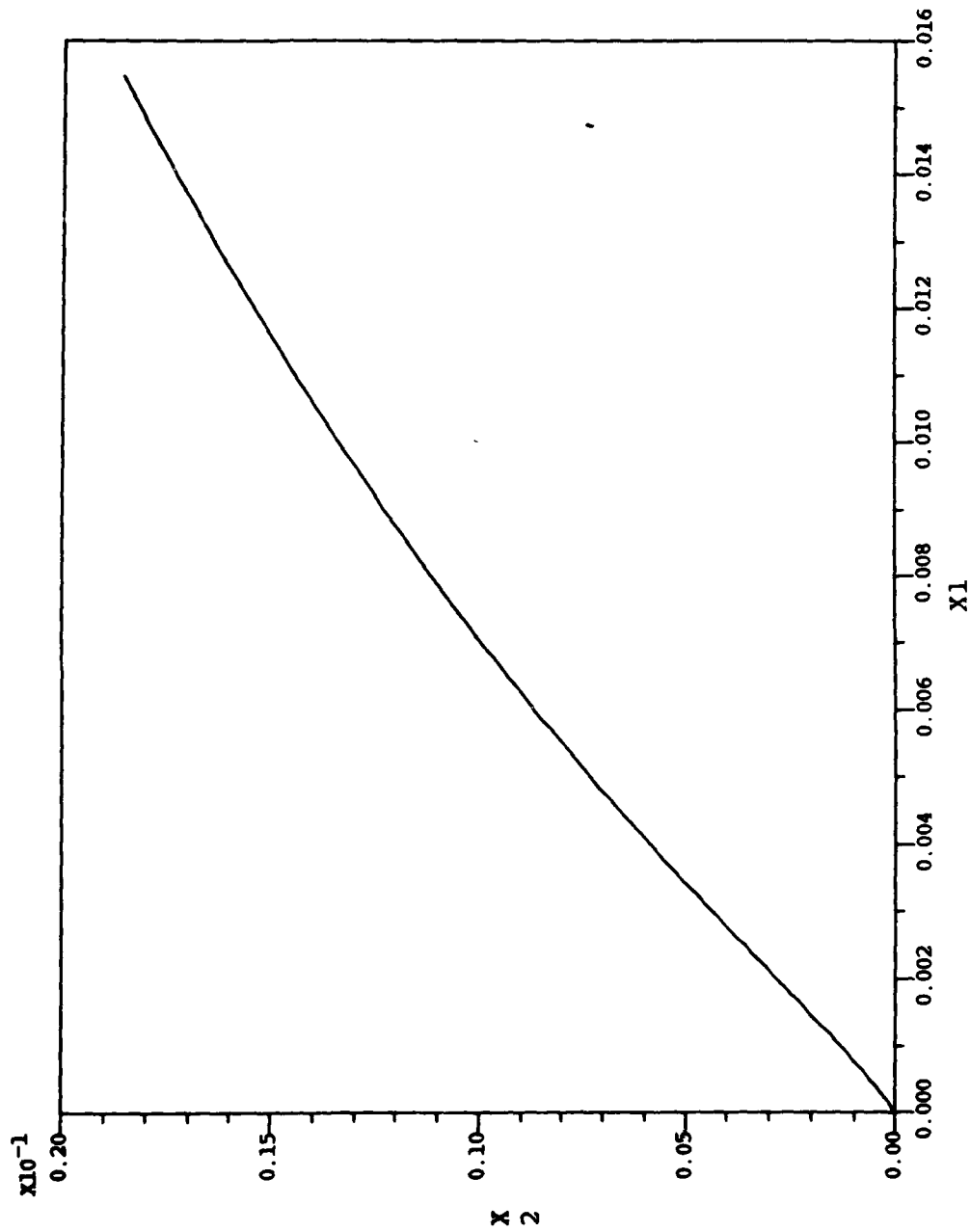


Fig. 10. Trajectory for Case 2

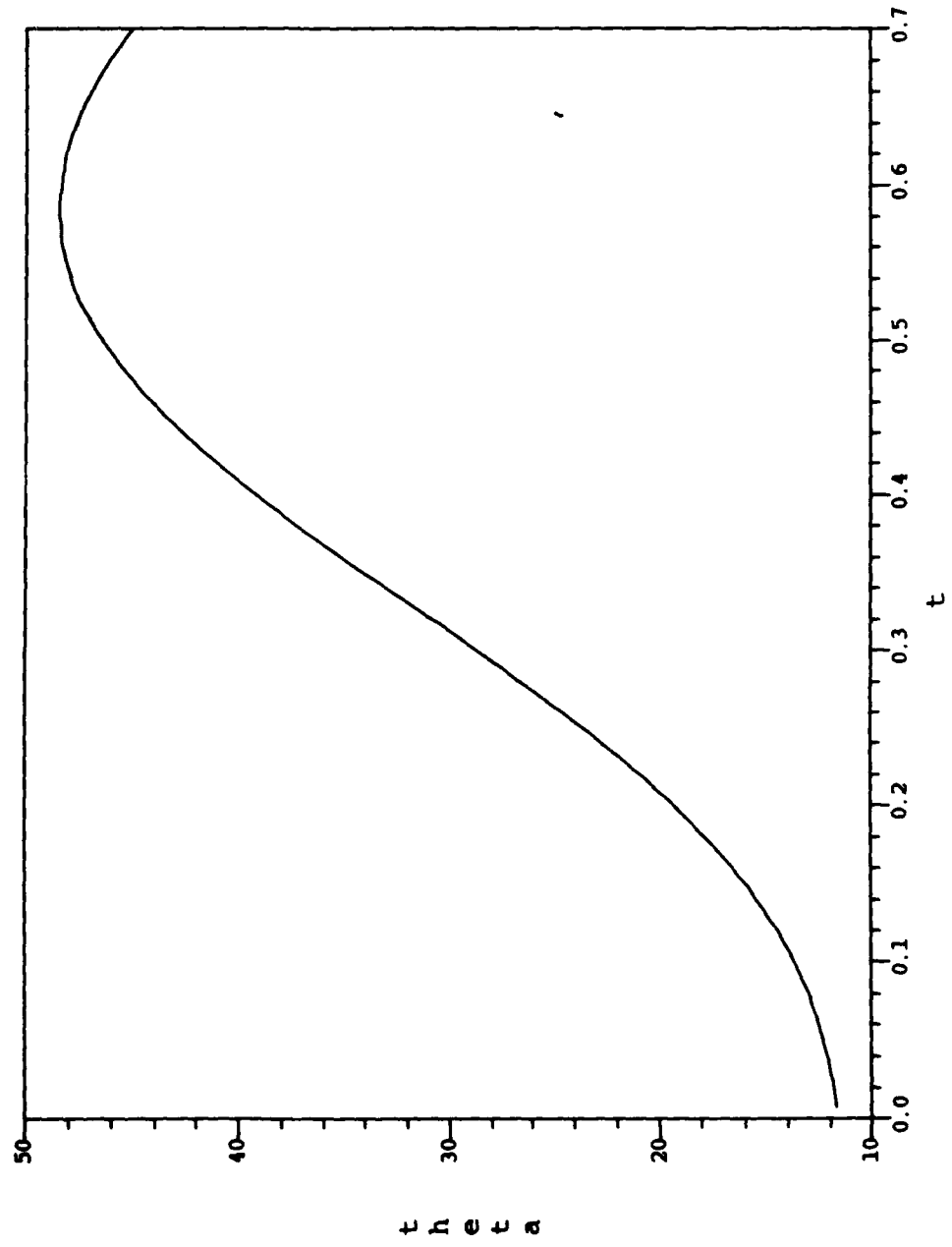


Fig. 11. Theta (degrees) vs Time for Case 2

t h e t a

Case 3

The purpose of Case 3 was to drive a spacecraft initially spiralling out from Earth to rest at L_2 . This case was chosen because an outward spiral is the optimal way to escape the primary in the two body problem for continuous low thrust. Since this spacecraft was spiralling out from Earth, the initial velocity corresponds to circular orbit velocity at the initial distance from Earth.

Values for F and t_f as well as initial costates were refined until after several forward and backward integrations, a converging trajectory was found. For this case, $F = 2.4$ and $t_f = 0.1044$, which corresponds to 10.9475 hours. The initial position was:

$$x_1 = 0.9369842 \times 10^{-3}$$

$$x_2 = 0.1298685 \times 10^{-1}$$

which puts the spacecraft 0.848128402 units or 326020.5577 km. from Earth. Circular velocity for this distance is 1.105658823 km/sec which is 1.085814904 units. This is the inertial velocity of the spacecraft at t_i and the velocity vector is perpendicular to the radius vector from the Earth to the spacecraft. This radius vector is at 179.1227348 degrees from the +x direction at t_i , so the initial inertial velocity expressed in the rotating frame is

$$v_x = -0.016624443$$

$$v_y = -1.085649737$$

Fortunately the conjugate momenta p_x and p_y turn out to be the inertial velocities of the spacecraft. Since $x_3 = p_x$ and $x_4 = p_y - x_L$, x_3 and x_4 become

$$x_3 = -0.016624443$$

$$x_4 = -0.248728034$$

Fig. 12 presents the trajectory and Fig. 13 presents θ vs time for this case. Along this trajectory, there were two eigenvalues which were nearly zero. This means changes to the initial costates along two null eigenvectors produce no change in the final states. This might be expected since the trajectory is integrated over a shorter time span so changes in the control would have less effect on the final states. The magnitude of gravity and Coriolis forces at t_i is 0.2449, (about one tenth of the thrust value).

Although this may not be low thrust by strict definition, it must be noted that at L_2 all forces cancel, so the stated definition breaks down near L_2 . $F = 2.4$ could actually be a very small thrust; for example, for a spacecraft of mass 15,447 kg., $F = 2.4$ is equivalent to 100 N of thrust.

Case 4

The purpose of Case 4 was to demonstrate that the linearized dynamics were valid in the vicinity of L_2 . For

Case 4, the initial conditions for Case 3 were translated back to the nonlinear states so that

$$x = -0.836036896$$

$$y = 0.01299080$$

$$p_x = -0.016625808$$

$$p_y = -1.085642753$$

and the same initial costates used. The full nonlinear dynamics [eqns.(32), (40)-(43)] were integrated from these initial conditions to $t_f = 0.1044$ with $F = 2.4$. The trajectory is shown in Fig. 14 and θ vs time is shown in Fig. 15. Fig. 14 indicates that the spacecraft does indeed go to L_2 as expected. Fig. 15 is identical to Fig. 13, therefore, the control applied in Case 3 and Case 4 was exactly the same. This demonstrates that the linearized dynamics were valid for Case 3.

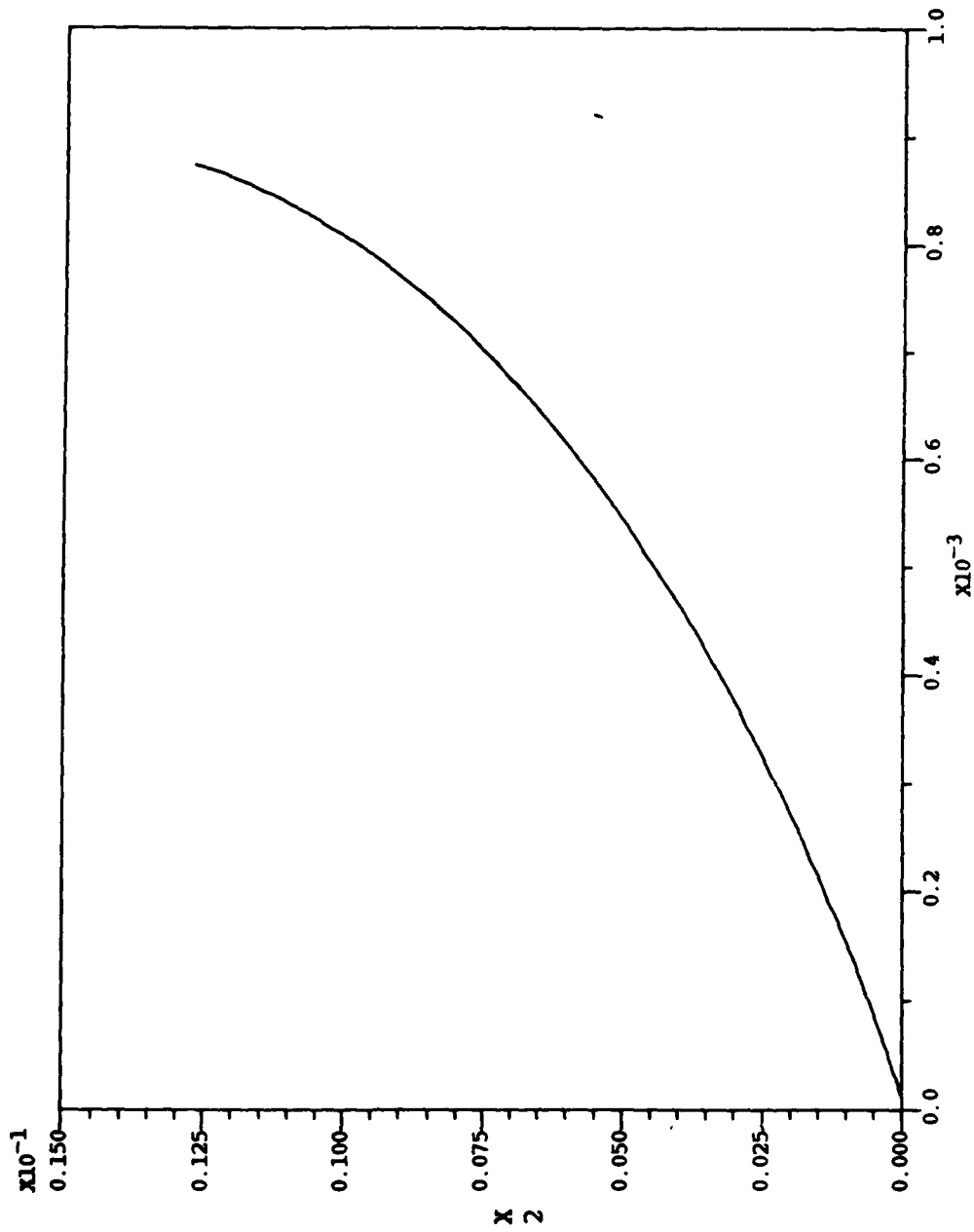


Fig. 12. Trajectory for Case 3

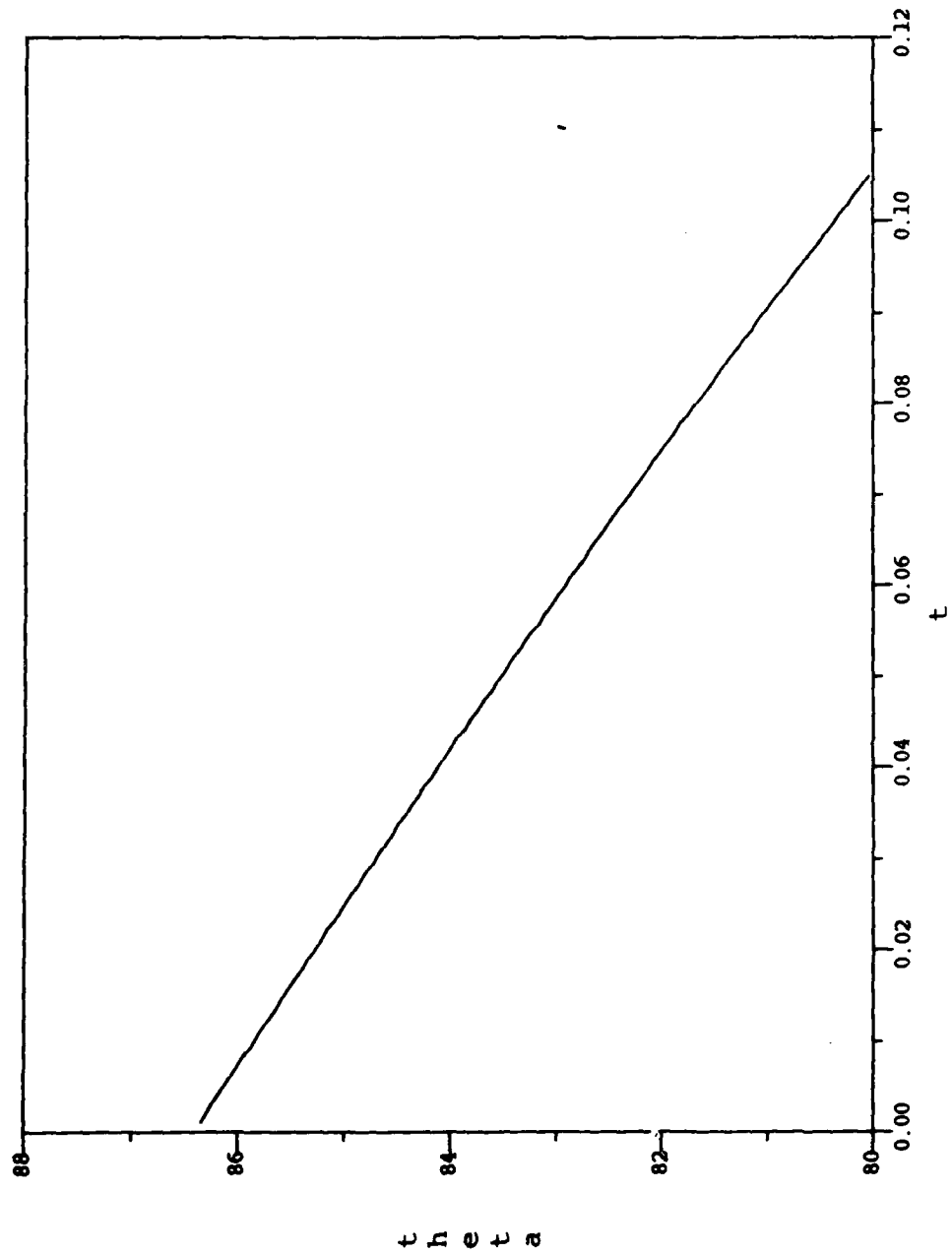


Fig. 13. Theta (degrees) vs Time for Case 3

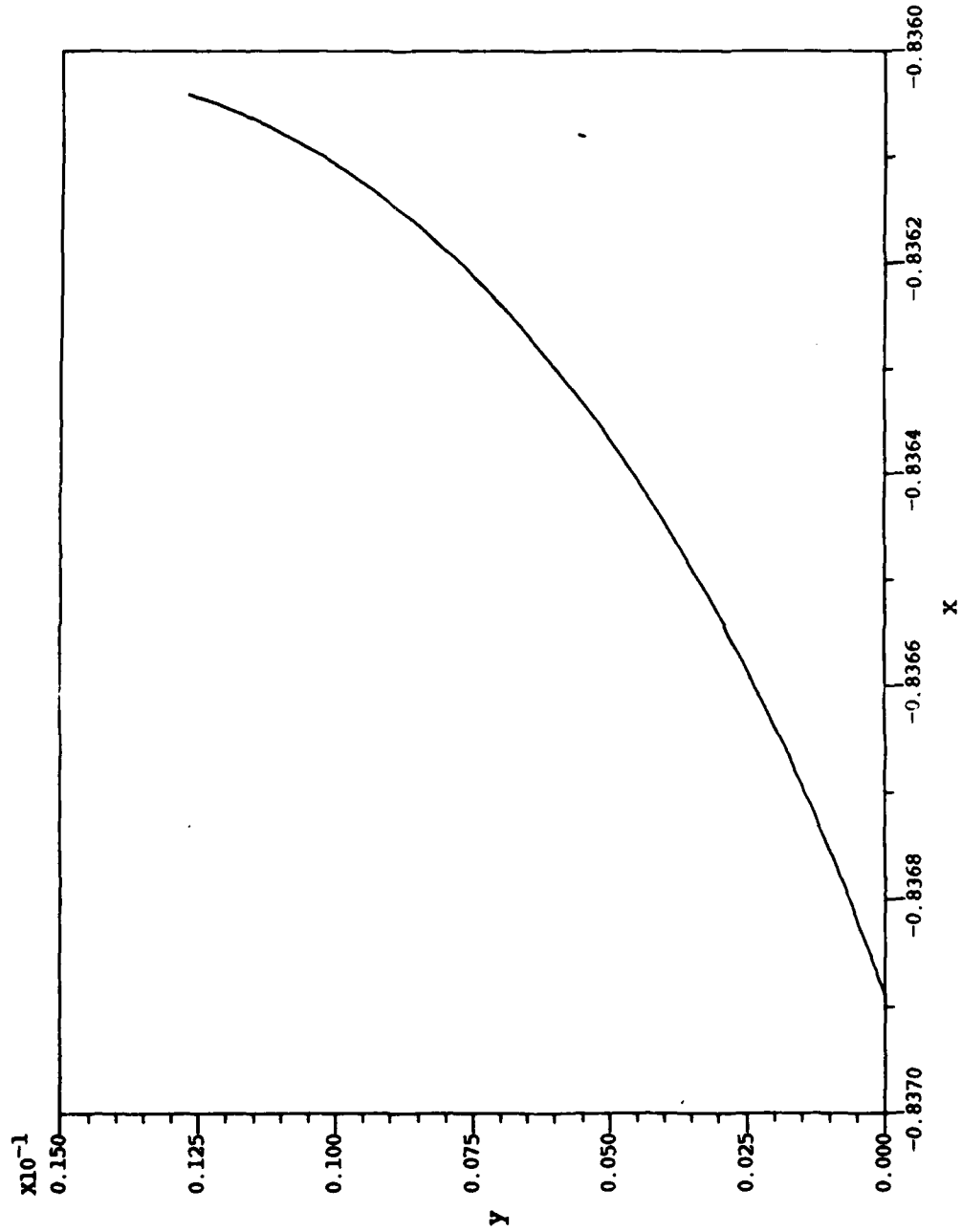


Fig. 14. Trajectory for Case 4

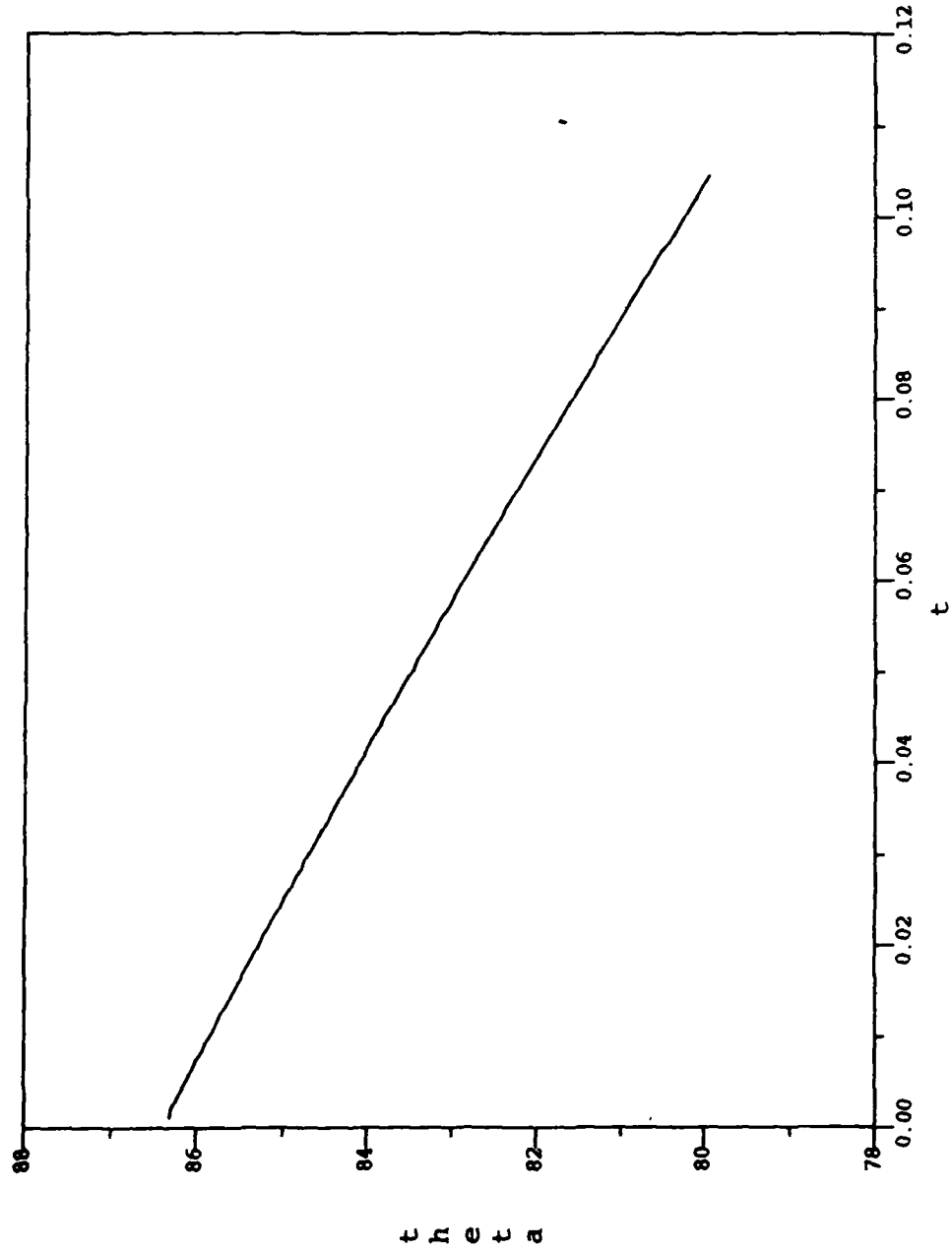


Fig. 15. Theta (degrees) vs Time for Case 4

IV. Conclusions

It has been shown that capture may be achieved by driving a spacecraft to rest at L_2 in the restricted three body problem. An optimal control law was developed to achieve this based on maximizing H . The resulting two point boundary value problem had no closed form solution, so a numerical solution was developed. The dynamics were linearized around L_2 for the Earth-Moon system and the shooting method was used to solve the two point boundary value problem.

This problem was singular so the shooting method was modified to avoid making corrections along the null eigenvector. Case 1 showed that the modified shooting method was able to solve the two point boundary value problem if the initial conditions were very close to the nominal initial conditions. Case 2 showed that the problem was indeed singular.

Case 3 drove a spacecraft which was spiralling out from Earth to rest at L_2 . Case 4 demonstrated that the linearized dynamics were valid for Case 3. Therefore the optimal control law successfully caused the spacecraft to be captured by the moon.

This study only looked at solving the two point boundary value problem for fixed final times. The

suggested next step would be to examine varying the final time to further optimize the trajectory. This could be done by finding the control Hamiltonian for two different final times and then using a secant method to find the final time which renders the control Hamiltonian equal to zero. This might be extremely difficult since the shooting method does not converge for this problem unless the initial conditions are almost exactly correct.

Bibliography

1. Bate, Roger R., Mueller, Donald D. and Jerry E. White. Fundamentals of Astrodynamics. New York: Dover Publications, Inc., 1971.
2. Bryson, Arthur E. Jr. and Yu-chi Ho. Applied Optimal Control. New York: Halsted Press, 1975.
3. Schultz, Donald G. and James L. Melsa. State Functions and Linear Control Systems. New York: McGraw-Hill, 1967.
4. Szebehely, Victor. Theory of Orbits. New York: Academic Press, 1967.
5. Wiesel, William E. Class notes distributed in MECH 731, Methods of Orbit Determination, Air Force Institute of Technology (AU), Wright-Patterson AFB, OH, May 1988.

VITA

Captain David E. Gaylor [REDACTED]
[REDACTED]
[REDACTED]

He received a Bachelor of Science in Astronautical Engineering from the United States Air Force Academy on 30 May 1984 and was commissioned. Upon graduation, he was assigned to the 6585th Test Group (AFSC), Holloman AFB, NM and served as an Inertial Navigation Systems Analyst until entering the School of Engineering, Air Force Institute of Technology, in June 1987.

[REDACTED]
[REDACTED]

REPORT DOCUMENTATION PAGE

1a. REPORT SECURITY CLASSIFICATION UNCLASSIFIED		1b. RESTRICTIVE MARKINGS	
2a. SECURITY CLASSIFICATION AUTHORITY		3. DISTRIBUTION / AVAILABILITY OF REPORT Approved for public release; distribution unlimited.	
2b. DECLASSIFICATION / DOWNGRADING SCHEDULE			
4. PERFORMING ORGANIZATION REPORT NUMBER(S) AFIT/EN/AA/88D-04		5. MONITORING ORGANIZATION REPORT NUMBER(S)	
6a. NAME OF PERFORMING ORGANIZATION School Of Engineering	6b. OFFICE SYMBOL (If applicable) AFIT/ENY	7a. NAME OF MONITORING ORGANIZATION	
6c. ADDRESS (City, State, and ZIP Code) Air Force Institute of Technology Wright-Patterson AFB OH 45433-6583		7b. ADDRESS (City, State, and ZIP Code)	
8a. NAME OF FUNDING / SPONSORING ORGANIZATION	8b. OFFICE SYMBOL (If applicable)	9. PROCUREMENT INSTRUMENT IDENTIFICATION NUMBER	
8c. ADDRESS (City, State, and ZIP Code)		10. SOURCE OF FUNDING NUMBERS	
		PROGRAM ELEMENT NO.	PROJECT NO.
		TASK NO.	WORK UNIT ACCESSION NO.
11. TITLE (Include Security Classification) OPTIMAL LOW THRUST TRAJECTORIES FOR PLANETARY CAPTURE (Unclassified)			
12. PERSONAL AUTHOR(S) David E. Gaylor, B.S., Capt, USAF			
13a. TYPE OF REPORT MS Thesis	13b. TIME COVERED FROM _____ TO _____	14. DATE OF REPORT (Year, Month, Day) 1988 December	15. PAGE COUNT 55
16. SUPPLEMENTARY NOTATION			
17. COSATI CODES		18. SUBJECT TERMS (Continue on reverse if necessary and identify by block number)	
FIELD	GROUP	Celestial mechanics, Capture, Three Body Problem	
22	03	Low Thrust Trajectories, Shooting Method	
19. ABSTRACT (Continue on reverse if necessary and identify by block number) Thesis Advisor: Dr. William E. Wiesel Professor of Astronautics The purpose of this study is to find optimal low thrust capture trajectories in the restricted three body problem. If the spacecraft is driven to rest at the equilibrium point L_2 , capture has been achieved by adding the least energy. An optimal control law is developed to achieve this based on maximizing the Jacobi integral. The dynamics are then linearized around L_2 for the Earth/Moon system and the shooting method is used to solve the two point boundary value problem. This problem is singular so the shooting method is modified to avoid making corrections along the null eigenvector. Four trajectories are presented which demonstrate the optimal control law successfully causes capture by the Moon.			
20. DISTRIBUTION / AVAILABILITY OF ABSTRACT <input checked="" type="checkbox"/> UNCLASSIFIED/UNLIMITED <input type="checkbox"/> SAME AS RPT. <input type="checkbox"/> DTIC USERS		21. ABSTRACT SECURITY CLASSIFICATION UNCLASSIFIED	
22a. NAME OF RESPONSIBLE INDIVIDUAL Dr. William Wiesel		22b. TELEPHONE (Include Area Code) (513) 255-3069	22c. OFFICE SYMBOL AFIT/ENY

Approved for release in accordance with AFR 200-100-100
 12 Jan 1989